J. Astrophys. Astr. (2013) **34,** 175–192

Generation of a Near Infra-Red Guide Star Catalog for Thirty-Meter Telescope Observations

Smitha Subramanian[1,*], Annapurni Subramaniam[1], Luc Simard[2], Kim Gillies[3], A. N. Ramaprakash[4], G. C. Anupama[1], C. S. Stalin[1], Swara Ravindranath[4] & B. Eswar Reddy[1]

[1] *Indian Institute of Astrophysics, Koramangala, Bangalore 560 034, India.*
[2] *National Research Council of Canada, Herzberg Institute of Astrophysics, 5071 West Saanich Road, Victoria, British Columbia, Canada.*
[3] *Thirty-Meter Project Office, Pasadena, California, USA.*
[4] *Inter-University Center for Astronomy & Astrophysics, Pune 411 007, India.*
e-mail: smitha@iiap.res.in

Received 15 March 2013; accepted 19 June 2013

Abstract. The requirements for the production of a near Infra-Red Guide Star Catalog (IRGSC) for Thirty Meter Telescope (TMT) observations are identified and presented. A methodology to compute the expected J band magnitude of stellar sources from their optical (g, r, i) magnitudes is developed. The computed and observed J magnitudes of sources in three test fields are compared and the methodology developed is found to be satisfactory for the magnitude range, $J_{Vega} = 16$–22 mag. From this analysis, we found that for the production of final TMT IRGSC (with a limiting magnitude of $J_{Vega} = 22$ mag), we need g, r, i bands optical data which go up to $i_{AB} \sim 23$ mag. Fine tuning of the methodology developed, such as using Spectral Energy Distribution (SED) template fitting for optimal classification of stars in the fainter end, incorporating spectral libraries in the model, to reduce the scatter, and modification of the existing colour–temperature relation to increase the source density are planned for the subsequent phase of this work.

Key words. Stars—near infra-red magnitudes—adaptive optics.

1. Introduction

Thirty Meter Telescope (TMT) is an advanced, wide field (20 arcmin), altitude-azimuth telescope with a primary mirror consisting of 492 individual hexagonal segments, each 1.44 m in size. The telescope is planned for installation on the summit of Mauna Kea on the island of Hawaii in the United States.

At first light, a Multi-Conjugate Adaptive Optics (MCAO) system will be available using a Laser Guide Star (LGS) system. The facility's twin Nasmyth platforms will concurrently support multiple instruments, all of which will be available during the night for observations. Two science instruments will be delivered for use with the MCAO-LGS system: IRIS, a near infra-red instrument with parallel imaging and integral-field-spectroscopy support; and IRMS, an imaging, multi-slit near infra-red instrument. A seeing-limited, wide-field, multi-object optical imaging spectrograph (MOBIE) will also be available at first light. Narrow Field Infra-Red Adaptive Optics System (NFIRAOS) is the TMT's Adaptive Optics (AO) system for infra-red instruments. A schematic diagram of the NFIRAOS is shown in Fig. 1.

The main purpose of AO is to compensate for natural atmospheric turbulence in order to approach the theoretical diffraction limit. An adaptive optics system tries to correct the distortions, using a Wave Front Sensor (WFS) which takes some of the astronomical light, a deformable mirror that lies in the optical path, and a computer that receives input from the detector. A science target is often too faint or extented to be used as a reference star for measuring the shape of the optical wave fronts. A nearby brighter guide star can be used instead. But, sufficiently bright stars are not available in all parts of the sky, which greatly limits the usefulness of natural guide star AO. Instead, one can create an artificial guide star by shining a laser into the atmosphere. However, much fainter natural reference stars are still required for image position information. The TMT Infra-Red Guide Star Catalog (TMT-IRGSC) is a star catalog consisting of point sources with JHK$_s$ magnitudes as faint as 22 mag in J band, covering the entire TMT-observable sky from +90 to −45 degrees declination. The TMT-IRGSC will be a critical resource for TMT operations that enables efficient planning and observing, fulfilling a role similar to that of the Guide Star Catalog I and II, which were created to enable acquisition and control of the Hubble Space Telescope. No catalog currently exists with objects as faint as

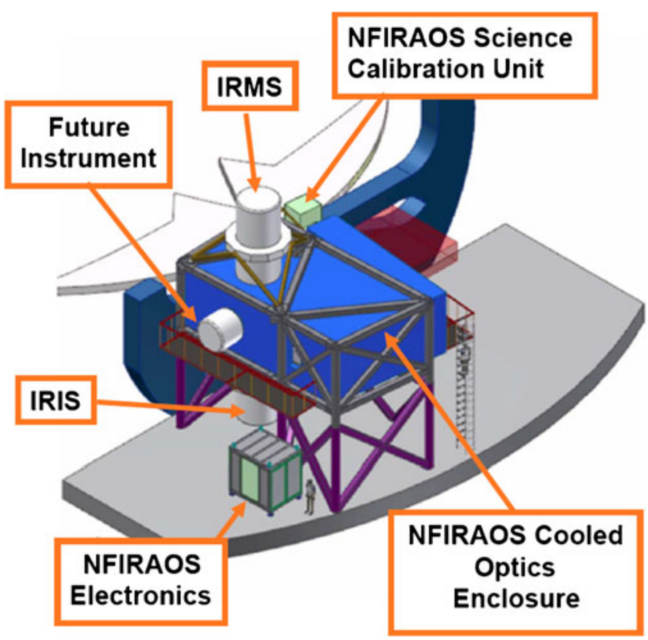

Figure 1. Schematic diagram of the NFIRAOS.

$J_{Vega} = 22$ mag over a large enough area of the sky to be useful as a guide star catalog. Hence it is highly essential to develop this catalog by computing the expected near infra-red magnitudes of sources using the optical magnitudes.

The scope of the present work is to identify the requirements for the generation of guide star catalog and hence to create a road map for the final production of TMT IRGSC. The structure of the paper is as follows. In section 2 the initial catalog requirements are identified. The availability of the optical data for the generation of the catalog is discussed in section 3. In section 4 a methodology developed for the computation of expected J band magnitude of probable stellar sources is described and the application of the methodology in different test fields are discussed in section 5. The results and discussion are given in section 6. The present work is summarized in section 7 and the plans for the next phase of the project are given in section 8.

2. Catalog requirements

The initial catalog requirements are analysed below.

(a) *Point sources*. The WFS algorithm requires point sources as guide stars. Point sources can be stellar and non-stellar (quasars, AGN etc) sources. For computing the expected magnitudes from optical magnitudes, the point sources should be stellar sources.
(b) *Multiple stars*. Information about the multiple stars present in the catalog should be included. Given that the IR GSC will be mostly constructed from ground-based data, it will not be possible to obtain the multiple star orbital parameters. However, we will be able to use Spectral Energy Distribution (SED) and magnitude to identify them. One component of the multiple star system can be used for guiding. At diffraction limit, we could identify the shift in positions of the stars. This will introduce an error that should be avoided. Multiple stars should be kept and flagged as multiples in the catalog.
(c) *Catalog Coverage*. The IR GSC should provide coverage for the entire sky that is observable by TMT in Hawaii. This is bounded by declination 90 degrees North and 45 degrees South. The optical data from the Canada France Hawaii Telescope (CFHT), Subaru's HyperSuprimeCam (which are situated in the same site as that of the proposed TMT site) and the data from all sky surveys like Panoramic Survey Telescope And Rapid Response System (Pan-STARRS) satisfy the coverage criteria and can be used for the production of the IR GSC for TMT observations.
(d) *Positional accuracy*. The field of view of WFS is 4 arcsec. The positional precision is based on astrometric requirements, as the guide stars are planned to be used as reference stars for absolute astrometric measurements. For that we need to reach to the order of milli-arc sec precision in positions.
(e) *Proper motion*. The proper motion information of the catalog stars are required. We plan to derive this information from multi-year surveys such as PAN-STARRS.
(f) *Magnitudes and colors*. The fainter end of the catalog should be J = 22 mag in the Vega system. The accuracy of the JHK_s magnitudes, especially in the fainter end has to determined.

(g) *Source density*. NFIRAOS requires 3 guide stars within its 2 arc min corrected field of view. These guide stars do not have to be within the imaging science field (which is 17 arcsec $\times$ 17 arcsec for IRIS). They can be chosen from the entire 2-arcmin NFIRAOS field.
(h) *Catalog object names*. Each entry should have a catalog-unique name following IAU naming conventions (e.g., TMTGSCJ06451-1643). It may be desirable to cross-reference an object to other existing catalogs.

3. Identification of fields with optical data for catalog production

As an initial step, the CFHT MegaPrime source material was identified and collected. One of the large survey programs of the CFHT was the CFHT Legacy Survey (CFHTLS). The CFHTLS was a more than five-year (May 2003–February 2009) duration large observing program at the CFH Telescope, using the wide field prime focus MegaPrime equipped with MEGACAM, a 36 CCD mosaic camera. Together with its small pixel scale of 0.185 arcsec and the large number of nights dedicated to the survey (around 500 nights over five years), the CFHTLS goes deeper and has a better image quality than the Sloan Digital Sky Survey (SDSS), but on a much smaller area of the sky.

The CFHTLS consists of three different surveys:

1. *The Deep*, a survey comprising four fields (named D1, D2, D3, D4) of 1 square degree each, in five filters u^*, g, r, i and z, reaching r up to 28 mag, observed every 3–4 days.
2. *The Wide*, a survey of 4 patches (W1, W2, W3, W4) in five bands, with limiting magnitudes r up to 25 mag, observed in two epochs separated by 3 years. This covers around 170 square degrees in the sky.
3. *The Very Wide*, a survey of 1300 square degrees along the ecliptic, on 5–6 epochs, dedicated to the detection of fast moving solar system objects and stellar populations.

The 6th data release of the CFHTLS comprises of the all planned CFHTLS Deep (4 square degrees in the sky) and Wide (152 square degrees in the sky) scientific observations. The catalog (Gwyn 2011) is split by band and by pointing. To increase the user friendliness, the individual catalogs are now merged to form a unified catalog. Each merged catalog contains measurements in all 5 of the u^*g, r, i, z Mega Cam filters and covers an entire survey (either the Wide or the Deep). Separate catalogs were generated using each of the 5 bands as a reference/detection image. Thus there is an u-selected, g-selected, r-selected, i-selected and z-selected catalog for each survey, each suiting to different science goals (for e.g. i-selected for general galaxy population studies, z-selected if you are looking for i-band dropouts, etc.). Although the catalogs are selected in a single filter, measurements are made in all 5 filters for each catalog, removing the need to consult multiple catalogs. There are thus a total of $5 \times 2 = 10$ separate catalogs, each complete in itself, but with different detection characteristics. The data files can be downloaded from, http://www3.cadc-ccda.hia-iha.nrc-cnrc.gc.ca/community/CFHTLS-SG/docs/catdoc.html.

More optical MegaPrime source material observed using CFHT can be obtained from the MegaPrime archive, http://www4.cadc-ccda.hia-iha.nrc-cnrc.gc.ca/cadcbin/cfht/wdbi.cgi/cfht/quick/form. MegaPipe archive contains fully-reduced, stacked images of everything in the MegaPrime archive. See http://www3.cadc-ccda.hia-iha.nrc-cnrc.gc.ca/megapipe/. In future, the optical (g, r, i) data from Pan-STARRS (all-sky survey) and from HyperSuprime Cam on the 8.2 m Subaru telescope (in Hawaii which makes the observable sky similar to that of TMT) can be used for the production of TMT IR GSC. But the typical limiting magnitude of Pan-STARRS is ∼24 mag which is not as deep as MegaPrime data. By adding observations taken over several years, Pan-STARRS should be able to reach a maximum depth of magnitude 29.4. Hyper Suprime-Cam (HSC) was installed on the Subaru Telescope in August 2012. Combined with the superb image quality and large aperture of Subaru telescope, the survey using HSC can cover a cosmological volume and reach the limiting magnitude of at least one magnitude fainter than other surveys conducted using 4-m class telescopes. Thus the data from HSC can go one magnitude fainter than CFHT data. But it is unclear what the sky coverage of the HSC data will be over the next few years.

We now discuss the development of an appropriate methodology for the computation of the J band magnitudes of the stellar sources from their optical (g, r, i) magnitudes.

4. Development of a methodology to compute the J band magnitude

The first step is to identify probable stellar sources from the optical catalogs. Then we have to estimate the temperature of the stellar source from the optical colour, and then assume a model to estimate the flux emitted by the source in different band widths. The model is used to compute the absolute flux in optical bands and then compare with observed optical fluxes to estimate the scaling factor, which is a measure of the distance to the source. The estimated scaling factor is used to compute the expected flux in the J band as observed from the Earth and eventually the magnitude in the J band. The steps involved are described below in detail.

4.1 *Identification of probable stellar sources*

As an initial step, the probable stellar sources can be identified based on the stellar/galaxy flags given in the optical catalogs. In general stellar sources are flagged based on their extend. The criteria used to identify probable stellar sources is based on the locus in magnitude vs. half-light radius plot. Such a plot is shown in Fig. 2. The blue points are the stellar sources, red are spurious objects and the black are the galaxies. The blue line is the locus of the stars. On this plot, the galaxies occupy a range of magnitudes and radii while the stars show up as a well-defined horizontal locus, turning up at the bright end where the stars saturate. So the sources in the stellar locus, fainter than 17 magnitude (basically those occupy the horizontal locus) can be considered as stellar sources.

This kind of classification based on spatial extent is only an initial step for the identification of probable stellar sources. The classification based on ground-based imaging data is not good enough for TMT. Because, at its higher resolution, the

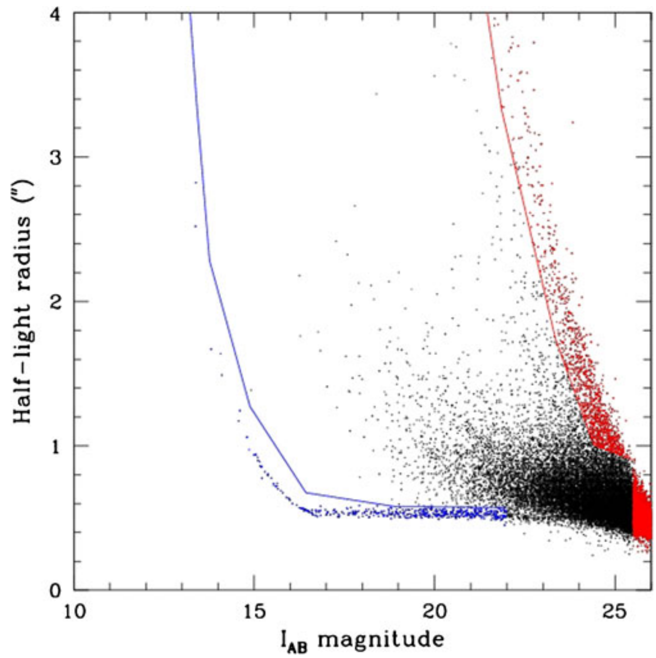

Figure 2. I_{AB} mag vs. half-light radius plot of all the sources in CFHTLS field. The blue points are the stellar sources, red are spurious objects and the black are the galaxies. The blue line is the locus of the stars.

source which is classified as point source only based on its spatial extent from lower resolution data may turn out to be an extended source. Also, the selection criteria used here cannot do an optimal star/galaxy classification in the fainter end (fainter than 22 mag in the I band). Thus sources fainter than 22 mag in the I band in our sample are removed. From this sample we can only get stars up to ∼20 mag in the J band. This is not appropriate for the final TMT IRGSC, which should have stellar sources up to 22 mag in the J band. For the optimal classification, we have to use Spectral Energy Distribution (SED) template fitting procedure for the sources in the test field. The SED template fitting procedure for the optimal selection of stellar sources from the optical data is planned in the subsequent phase of this work.

4.2 *Estimation of the temperature of the stellar source*

Empirical and theoretical colour–temperature relations for different photometric bands are derived by various groups. The early authority of the colour–temperature relation is the one given by Johnson (1966). The work prior to 1980 is summarized by Bohm-Vitense (1980). Later many people worked on this (Code *et al.* 1976; Bessell 1979; Ridgway *et al.* 1980; Arribas & Martínez Roger 1988; Tsuji *et al.* 1996; Flower 1996; Alonso *et al.* 1996; Blackwell & Lynas-Gray 1998; Lejeune *et al.* 1998; Sekiguchi & Fukugita 2000; Pinsonneault *et al.* 2004; An *et al.* 2007). Most of these were based on the Johnson Cousins system. In An *et al.* (2009) they used SDSS photometry of a solar-metallicity cluster M67 (An *et al.* 2008) to define a photometric u, g, r, i, z, $-T_{\text{eff}}$ relation, and checked the metallicity scale using star clusters over a wide range of metallicity. Lee *et al.* (2008) derived theoretical and empirical temperature estimates for the SDSS colours, during the execution of the SEGUE Stellar Parameter Pipeline (SSPP). Ivezic *et al.* (2008) found that a good correlation between the spectroscopic effective temperature and observed $(g - r)$ color extends beyond the restricted color range where the photometric metallicity method is applicable $(0.2 < (g - r) < 0.4)$. The colour–temperature relation which is valid in the colour range, $-0.3 < g - r < 1.3$ color range (roughly $-0.1 < B - V < 1.3$), given below is used for the estimation of the temperature of the stellar sources.

$$\log T_{\text{eff}} = 3.882 - 0.31(g - r) + 0.0488(g - r)^2 + 0.0283(g - r)^3.$$

The colour range corresponds to a temperature range $\sim$ 4200–9600 K. As no colour–temperature relation exists for the MegaPrime filters, we have to convert the MegaPrime magnitudes to SDSS magnitudes and then apply the colour–temperature relation mentioned above to estimate the effective temperature. We converted the $(g - r)_{\text{MegaPrime}}$ colour into $(g - r)_{\text{sdss}}$ colour using the color terms between the two filters which are given in Gwyn (2008). Those equations are solved to convert the $(g - r)_{\text{MegaPrime}}$ to $(g - r)_{\text{sdss}}$ which is then used to obtain the temperature of the source. The relation which converts the MegaPrime colour to SDSS colour is

$$(g - r)_{\text{sdss}} = 1.148106 * (g - r)_{\text{MegaPrime}}.$$

The observed dereddened colour is used to obtain the effective temperature. The relation used to deredden the $(g - r)_{\text{sdss}}$ colour is

$$(g - r)_{\text{dereddened}} = (g - r)_{\text{sdss}} - 1.042 * E(B - V).$$

4.3 *Determination of scaling factor from the optical magnitudes*

In the present study, stars are approximated as black bodies. The absolute flux of each source (with temperature T) in any band can be estimated by integrating the Planck's black body equation within the corresponding pass band. Once the temperature is estimated we can compute the absolute flux of the source in the J band (n1 to n2 where n1 and n2 are the lower and upper band pass of the filter).

$$\text{Absolute flux in a band} = \int_{n1}^{n2} 2hn^3(\mathrm{e}^{hn/kT} - 1)^{-1}/\mathrm{c}^2 \mathrm{d}n.$$

The absolute flux obtained by integrating the Planck's function has unit of erg/s/cm^2/Sr. But in order to convert the absolute J band flux to the observed/apparent flux we should know the solid angle subtended by the source to the detector. The solid angle goes as $1/r^2$, where r is the distance to the source. But it is not possible to get the distances to all the sources in a field. An alternate method is to get the scaling factor from the known optical magnitudes. The absolute flux in any band can be computed by integrating the Planck's function within the band width of the filter. From the observed magnitudes, observed flux can be estimated. Comparing the observed and computed fluxes, the scaling factor can be calculated. The flux from the source received at the Earth is measured using a system consisting of optics, mirror, filter and CCD. The observed flux will have the effect of the system response. In order to estimate the actual scaling factor, the absolute flux computed should be convolved with the same response function. The response of the system for each band has to be taken into account while computing the absolute flux. For that, while integrating, the Planck's function is convolved with the response function of the system. Again this response function has to be taken into account while calculating the effective band width which is required to obtain the specific flux (the flux per unit frequency). The formula to obtain the absolute specific flux after incorporating the system response is given as

$$\text{Absolute specific flux in a band} = \int_{n1}^{n2} R(n) 2hn^3 c^{-2} (e^{hn/kT} - 1)^{-1} dn \Big/ \int_{n1}^{n2} R(n) dn$$

where $R(n)$ is the response of the system as a function of frequency. The above quantity has units of erg/s/cm^2/Sr/Hz. The absolute specific flux after incorporating the response of the system in the optical bands g, r, i (F_g, F_r and F_i) are calculated as described.

In order to calculate the scaling factor, the observed flux in the g, r, i bands are required. From the extinction corrected optical magnitudes, flux in g, r and i bands, f_g, f_r and f_i are calculated.

The scaling factor is the ratio between the system response corrected absolute flux and the observed flux of the source. The scaling factors using the g, r and i band fluxes are estimated.

Scaling factor obtained from g band, $Sg = F_g/f_g$,
Scaling factor obtained from r band, $Sr = F_r/f_r$,
Scaling factor obtained from i band, $Si = F_i/f_i$.

In principle, the scaling factors obtained from different bands should be the same. An average of the scaling factors obtained from the 3 bands can also be used in the conversion of system response corrected absolute J band flux to observed J band flux.

4.4 *Computation of the J band flux and magnitude*

For the production of TMT IRGSC, we need to compute the expected J band magnitude as observed through the TMT. The absolute specific flux in the J band has to be calculated after incorporating the response function of the TMT. Then the average scaling factor obtained from the optical bands will be used to estimate the apparent J band flux. The apparent J band flux estimated is converted to J magnitude in Vega system using the zero magnitude flux given in Bessell *et al.* (1998). The computed J band magnitudes will then be reddened using the relation

$$J_{\text{reddened}} = J_{\text{computed}} + 0.8215 * E(B - V).$$

Thus the expected J band magnitude of sources as observed through TMT is estimated.

5. Validation of the developed methodology

In this section the identification of test fields and the application of the developed methodology in the identified test fields are described.

5.1 *Identification of appropriate test fields*

The criteria for an appropriate test field are:

(a) The test fields should have deep optical data which can be used to compute the J band magnitudes (up to 22 mag).
(b) It should have J band observations which will help to compare the observed and computed magnitudes and hence improve the methodology.

The CFHTLS deep fields are the appropriate choice for the test fields, as they have both deeper optical data and NIR observations. The NIR observations of the CFHTLS deep fields are done as part of the WIRcam Deep Sky Survey (WIRDSS). The WIRDSS observed the sub-sections of CFHTLS deep fields (D1, D3 and D4) and the full D2 deep field. WIRcam is a wide-field infrared camera in CFHT and it consists of four 2048 × 2048 HgCdTe arrays arranged in a 2 × 2 format, with gaps of 45 between adjacent chips. The detector pixel scale is 0.3/pixel resulting in a field-of-view of 21 × 21. The WIRDSS observed 2.4 square degree of the sky. The WIRDSS survey is designed to reach AB magnitudes of 24 in all near infra-red bands. The J band observations of D2 region was taken using WFCAM in UKRIT. Recently, Bielby *et al.* (2012) merged WIRcam deep survey data with CFHTLS data to obtain a catalog in which the data of the eight bands (u, g, r, i, z, J, H, K) of the sources are available. We use this merged catalog, especially that of the D2 field which has both optical and NIR data for the full 1 square degree field for the development and testing of the methodology. Thus D2 field is chosen as the test field, T1.

Though deep fields are the best test fields in the process of the development of the methodology, wide fields have more coverage and hence more data. The depth reached for each pointing of the wide-field survey is approximately: $u^* = 26.4$ mag, $g = 26.6$ mag, $r = 25.9$ mag, $i = 25.5$ mag, $z = 24.8$ mag. The depth is sufficient enough for the production of the TMT IR GSC. So we looked for wide-field regions which have J band observations to consider them also as test fields. To obtain the J band data of sources in the wide field observed regions of CFHTLS, we checked for the overlap of United Kingdom Infra-red Deep Sky Survey (UKIDSS) survey regions. The survey instrument is the Wide-Field Camera (WFCAM) on the United Kingdom Infra-red Telescope (UKIRT). The camera has four Rock-well Hawaii-II 20482 PACE arrays, with pixel scale 0.4, giving a solid angle of 0.21 square degree per exposure. The wide fields, W1 and W2 of the CFHTLS are not in the survey region of any of the surveys under UKIDSS. Sub-regions of the fields W3 and W4 come under the survey region of Large Area Survey (LAS). The W3 field data are, as yet, unavailable. Out of 25 sub-fields (1 × 1 square degree) of W4 field of the wide-field survey of CFHTLS around 9 fields have complete overlap with the LAS observed regions and 5 fields have partial overlap with the LAS observed regions. Out of the 9 sub-fields of W4 which have complete over-lap with LAS, 6 fields have complete overlap with another UKIDSS survey, known as Deep Extra galactic Survey (DXS). The limiting magnitude in the J band for the LAS is 20 mag. The limiting magnitude of DXS in the J band is 22 mag. So it is appropriate to consider the sub-regions of W4 which have DXS data. From such 6 sub-fields, we chose a 1 × 1 square degree field as the second test field (T2). Also another sub-field of W4 which has only LAS data is also chosen as third test field (T3) in order to check the procedure in a different environment. By cross matching the optical and NIR data from DXS and LAS accordingly for these test fields (the details are given in the analysis section of each test field), we created a merged catalog of sources in these sub-regions. The UKIDSS data is available from http://surveys.roe.ac.uk/wsa/startHere.html.

5.2 *Identification of probable stellar sources*

The probable stellar sources in all the three test fields are identified based on the stellar/galaxy flags given in the CFHTLS catalog of deep and wide fields. The stellar sources are flagged as 1 in the catalogs. The criteria used to identify probable stellar sources is explained in section 4.1. This selection criteria cannot do an optimal star/galaxy classification in the fainter end, beyond $I_{AB} \sim 21$ mag. So the sources which occupy a horizontal locus (stars in the i_{AB} magnitude range of ∼17–21 mag and half light radius less than ∼0.5 arcsec) are flagged as stars in the CFHTLS catalogs and we use them for further analysis. This kind of classification based on ground-based imaging data is not good enough for TMT. Because, at its higher resolution, the source which is classified as point source only based on its spatial extent from lower resolution data may turn out to be an extended source. For an optimal classification, we have to use SED template fitting procedure. This optimal selection of stellar sources from the optical data is planned for the subsequent phase of the project.

In the test field, T1 (which is a deep field) the number of probable stellar sources with optical and NIR magnitudes are 1882. Similarly in the test fields, T2 and T3 the number of probable stellar sources with NIR counterparts are 7717 and 6284 respectively. The test fields, T2 and T3 are from wide field regions.

5.3 *Computation of the expected J band magnitude*

The methodology developed in section 4 is applied to compute the expected J band magnitude of the probable stellar sources in the three test fields. First of all, the effective temperature of the stellar sources in the test fields are estimated using the colour temperature relation given in section 4.2. For the estimation of effective temperature, the observed colours are dereddened. The $E(B-V)$ of the sources in the T1 field is given in the optical catalog. From the maps (Schlegel *et al.* 1998) average reddening towards the test fields T2 and T3 are found. We found an average reddening, $E(B-V)$ of 0.06 mag and 0.05 mag towards T2 and T3 respectively. The applicable range of $(g-r)$ colour of the colour–temperature relation, reduced the number of sources in the test fields and hence the source density per field. In test field, T1, out of 1882 sources temperature could be estimated only for 868 sources. Similarly, for the test fields, T2 and T3 temperature was estimated only for 1813 and 2013 sources respectively.

The estimated temperature is used to compute the fluxes. The absolute specific flux after incorporating the response of the system in the MegaPrime optical bands g, r, i (F_g, F_r and F_i) are calculated as described in section 4.2. The response functions for MegaPrime bands are given as tables in the http://www3.cadc-ccda.hia-iha.nrc-cnrc.gc.ca/mega-pipe/docs/filters.html. In order to calculate the scaling factor, the observed flux in the g, r, i bands are required. The MegaPrime g, r, i magnitudes are in AB mag system. They are converted into flux per frequency using the equation given in Oke (1974).

$$\text{AB mag} = -2.5 \log(f_n) - 48.6.$$

The quantity f_n is the observed flux per frequency. The observed magnitudes are corrected for interstellar extinction before estimating the observed flux. The extinction co-efficient for the MegaPrime g, r, i bands were not available. So the extinction co-efficient for the SDSS g, r, i bands (Girardi *et al.* 2004) are used:

$$\begin{aligned} g_0 &= g - 3.773 * E(B - V), \\ r_0 &= r - 2.750 * E(B - V), \\ i_0 &= i - 2.086 * E(B - V). \end{aligned}$$

From the extinction corrected optical magnitudes, observed flux in g, r and i bands, f_g, f_r and f_i are calculated. By comparing the observed and computed fluxes, the scaling factor corresponding to each band are estimated. For all the stellar sources in the test fields scaling factors in all the bands are calculated. Though the scaling factors obtained from different bands are not exactly the same, they are more or less the same. The average of the three scaling factors are also used for the conversion of absolute J band flux to expected flux as observed from the Earth.

The absolute specific flux in the J band width is calculated after incorporating the response function. As we have to compare the computed magnitude with the observed magnitude using the WFCam, the response function of WFCam (Hewett *et al.* 2006) is used in the estimation of the absolute specific flux. Then the average scaling factor obtained from the optical bands is used to convert the response corrected absolute specific J band flux to the apparent flux. From the computed apparent J band flux, reddened J band magnitude is estimated as described in section 4.4.

5.4 *Comparison with the observed J magnitude*

The observed J magnitude of the 868 sources in the test field T1 are in AB magnitude system and the 1813 and 2013 sources in the test fields T2 and T3 respectively are in Vega magnitude system. The AB magnitude of sources in T1 are converted into Vega magnitude using the relation (Blanton & Roweis 2007),

$$J_{\text{Vega}} = J_{\text{AB}} - 0.91.$$

The computed J band magnitudes which are reddened are compared with the observed magnitudes. As mentioned in the previous section the sources in the test field are reddened using the $E(B - V)$ values given in the optical catalog. For the sources in T2 and T3 average reddening towards the fields taken from maps are used (Schlegel *et al.* 1998). Figure 3 shows the difference in the computed and observed magnitudes plotted against the observed magnitudes for the test field, T1. In order

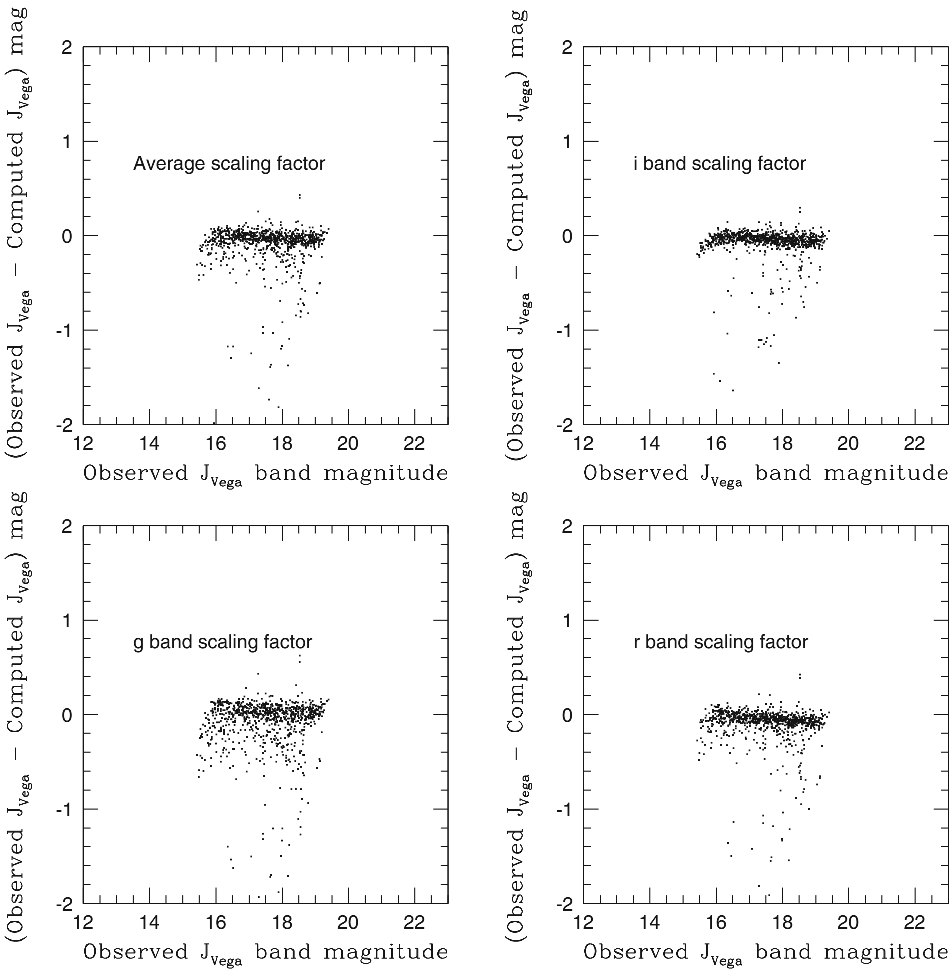

Figure 3. For the probable stellar sources in test field, T1 the difference between the observed and computed magnitudes are plotted against the observed J_{Vega} magnitude.

to check the dependence of scaling factors obtained from different bands, we plotted the computed magnitudes using the scaling factors from different bands also against the observed magnitude. Similar plots (Fig. 4 and Fig. 5) for the test fields, T2 and T3 respectively are also shown.

The mean difference in all the plots is nearly zero with a mean scatter of 0.1 mag. The error associated with the computed magnitudes are estimated by propagating the errors associated in each step of calculation. The average 1 σ error is ~0.05 mag for all the test fields. The errors are larger for fainter magnitudes. The 2 σ error is of the order of scatter seen in the plots. The small differences and the slight slope may all be due to contribution of stellar absorption lines and aperture correction in the observed magnitudes. The sources which show a difference in the computed and observed magnitudes larger than 3σ error (~0.15 mag) are considered to be outliers, which are probably non stellar sources. There are a few number of outliers in all the

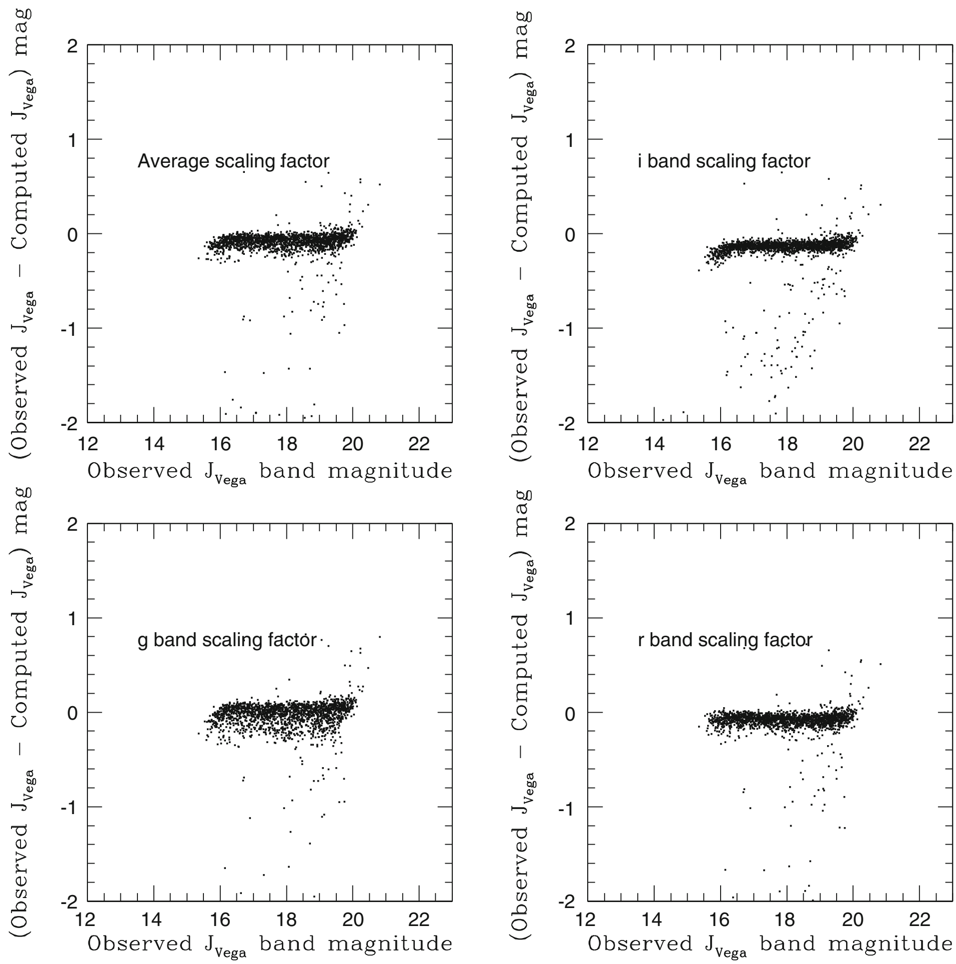

Figure 4. For the probable stellar sources in test field, T2 the difference between the observed and computed magnitudes are plotted against the observed J_{Vega} magnitude.

test fields, which may not be real stellar sources. The number of outliers in the test field, T3 (∼35%) are more compared to the other two test fields (∼18% and 14% in T1 and T2 respectively). Overall, the plots suggest that the methodology developed is appropriate and fine-tuning can be done to get more accurate results.

The computed magnitudes of most of the outliers are fainter than the observed magnitudes. The sources which show large deviation from the mean can be non stellar objects and their fluxes can be more than that estimated by assuming them to be stellar sources. The sources which show small deviation from mean can be real stellar sources. For these sources also most of them have computed magnitudes fainter than the observed magnitudes. Also, the mean difference between the observed and computed magnitudes is some cases is slightly shifted to the negative values. One of the probable reasons for this may be the fact that the model we use for stars do not incorporate the absorption features in the atmosphere of stars. We use a black body

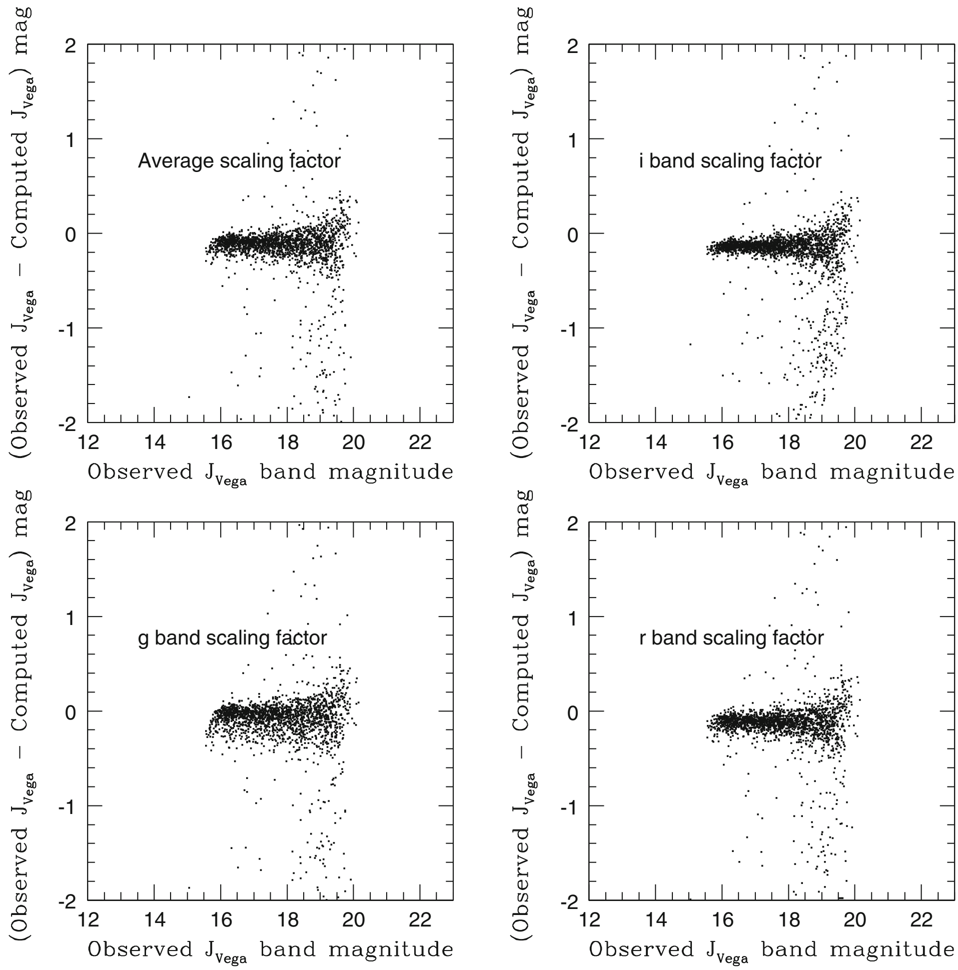

Figure 5. For the probable stellar sources in test field, T3 the difference between the observed and computed magnitudes are plotted against the observed J_{Vega} magnitude.

model to estimate the flux in each band. In reality, the stars do not act as perfect black bodies. There are absorption lines in the atmosphere of stars and that reduces the flux. Thus the flux computed in each band, based on black body model will be higher than the actual flux we receive from the star. The absorption features are more in the optical bands and it decreases in the infra-red bands. We use the computed optical fluxes to estimate the scaling factor, by comparing the computed with the observed. Thus the estimated scaling factor will be more than the actual one. This scaling factor is used to convert the computed absolute J band flux to the apparent J band flux. As the scaling factor is higher than the actual value, the computed flux will be less and hence the magnitudes will be fainter. As the absorption in the infra-red bands are very less the computed absolute flux is comparable with the actual one and so will not have significant effect on the computed magnitude. Thus the limitation in the model we use makes the computed magnitudes fainter. Hence the difference in the observed and computed magnitudes become negative. We plan to rectify this by using stellar atmospheric models for the computation of magnitudes, in the subsequent phase of the project. Another possibility is the uncertainty in the temperature estimates and reddening values. The computed magnitudes can be fainter than the observed one if the reddening values and temperatures are underestimated.

6. Results and discussion

The initial requirements for the TMT IRGSC are finalized. A methodology to compute the J band magnitudes of stellar sources from the optical magnitudes is developed by assuming a black body model for stars. For the validation of the methodology developed we computed the J band magnitudes of sources in three test fields and found that the observed and computed magnitudes match well. In Figures 3, 4 and 5 we can see that the computed $J_{\rm Vega}$ mag has a magnitude range of ∼16–20 mag. We do not have sources brighter than 16 mag because those sources are saturated in optical bands. The sources fainter than $J_{\rm Vega} \sim 20$ mag are also not available because the star/galaxy classification used here is not optimal for fainter sources. Thus the developed methodology is validated for the $J_{\rm Vega}$ mag range of 16–20 mag.

In order to check the validity of the developed methodology beyond these limits, we slightly extended the star/galaxy classification in the fainter end, (sources with $I_{\rm AB}$ up to 23 mag and half-light radius less than ~ 0.43 arcsec) and for these sources in the test field T2, the $J_{\rm Vega}$ mag are estimated. We cannot extend the classification criteria in the brighter end because the sources are saturated. The probable stellar sources with NIR counterparts in the test field T2 after applying the new classification criteria are 3584. For these sources the $J_{\rm Vega}$ mag are calculated and compared with the observed magnitudes. Figure 6 shows the difference in the observed and computed magnitudes of these sources plotted against the observed magnitudes. From the plot we can see that there are sources which show a mean difference of ∼ zero in the fainter end as well. These sources may be real stellar sources and we can assume that the methodology developed is valid till $J_{\rm Vega} \sim 22$ mag. But, when fainter sources are included by extending the star/galaxy classification, the number of outliers increased drastically to 37% of the sample. This is due to the contamination of non-stellar sources. For the optimal star/galaxy classification in the fainter end we have to use the SED template fitting technique. From this analysis, we also found that for the production of final TMT IRGSC (with a limiting magnitude of $J_{\rm Vega} = 22$ mag), we need sources with g, r, i bands optical data which goes as deep as $i_{\rm AB} \sim 23$ mag.

We also found that the source density criteria (3 stars in the 2 arcmin field of view) is not achieved in the test fields as the colour temperature relation we use is valid only for a particular range (4200 K to 9600 K) of temperature. When fainter sources are included in the test field T2 the source density criteria is satisfied. But we have to check it after incorporating the optimal star/galaxy classification. We may also need to derive/modify the existing colour temperature relation so that it is valid for a larger range of temperature and hence increase in the number of sources in the field.

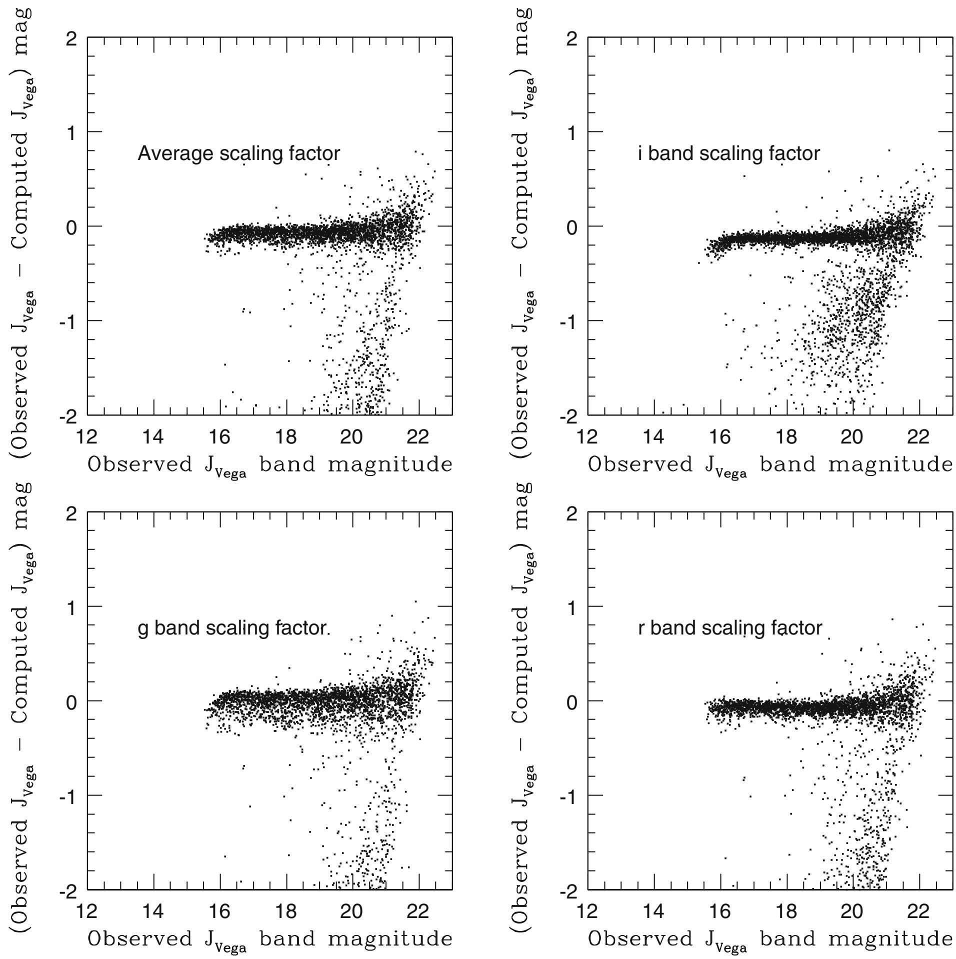

Figure 6. For the probable stellar sources (identified using the extended star/galaxy criteria) in test field, T2, the difference between the observed and computed magnitudes are plotted against the observed J_{Vega} magnitude.

Fine-tuning of the methodology developed, such as SED template fitting for optimal classification of stars, using spectral libraries (Pickles 1998) in the model, to reduce the scatter and modification of the existing colour–temperature relation to increase the source density are planned for the subsequent phase of this work.

7. Summary

(1) The catalog requirements are identified.
(2) A method to compute J band magnitudes from g, r, i magnitudes is developed.
(3) Summary of available data which can be used for the above purpose is provided.
(4) Three test fields from the above list are identified which can be used to test and validate the method developed.

(5) Method developed was found to be satisfactory (for the J_{Vega} range of 16–22 mag) as demonstrated by comparing the computed and observed magnitudes for three test fields.
(6) Factors which affect the adopted method are identified and methods for improvement are suggested. These are planned to be carried out in the subsequent phase of the project.

8. Plan for the next phase of the project

Main Objectives:

(1) *Classification of stellar sources*. Development and application of SED fitting method for the optimal classification. The star-galaxy classification criteria used has limitations. Even though the optical data goes deeper up to 25.5 mag in the I band, the optimal star-galaxy separation extends only up to 21 mag in the I band. This corresponds to an approximate J_{Vega} magnitude of 20. The requirement of TMT IR GSC is that it should go up to a limiting magnitude of $J_{Vega} = 22$ mag. In order to get the fainter stellar sources from optical data, a better classification based on SED fitting is required.
(2) *Computation of JHK$_s$ magnitudes of sources in the test fields*. Apply the methodology developed to compute the JHK$_s$ magnitudes of the stellar sources identified using SED fitting technique. The computed J, H and K$_s$ magnitudes have to be compared with the observed magnitudes. The final release, 7th release of the CFHTLS data Cuillandre *et al.* (2012) is now out. See http://terapix.iap.fr/cplt/T0007/doc/T0007-doc.html. In the present study, we used the 6th release data. In the subsequent phase of this work we plan to use the data from 7th release.
(3) *Fine-tuning of the methodology developed in the present study*. To incorporate the spectral libraries in the model. This will help to reduce the difference in the computed and observed magnitudes.
(4) *To create a road map for the final catalog*. Analyze thoroughly the entire procedure to check whether the existing data processing is adequate or, some extra/streamlined processing of data is needed to get the required parameters in the catalog. The steps to be taken, for the production of final IR GSC as the PANSTARRS and Subaru HSC data come in will also be analysed.

Acknowledgements

The authors are grateful to Prof. T. P. Prabhu for a critical reading of the document and for his valuable comments. We also thank Brent Ellerbroek and Matthias Schoeck for their inputs. One of the authors (SS) would also like to thank Ramya and Jessy for interesting discussions.

References

Alonso, A., Arribas, S., Martínez Roger, C. 1996, *A&AS*, **117**, 227.
An, D., Terndrup, D. M., Pinsonneault, M. H. 2007, *ApJ*, **671**, 1640.
An, D. *et al.* 2008, *ApJS*, **179**, 326.
An, D. *et al.* 2009, *ApJ*, **700**, 523.

Arribas, S., Martínez Roger, C. 1988, *A&A*, **206**, 63.
Bessell, M. S. 1979, *PASP*, **91**, 589.
Bessell, M. S., Castelli, F., Plez, B. 1998, *A&A*, **333**, 231.
Bielby, R., Hudelot, P., McCracken, H. J. *et al*. 2012, *A&A*, **545**, 23.
Blackwell, D. E., Lynas-Gray, A. E. 1994, *A&A*, **282**, 899.
Blackwell, D. E., Lynas-Gray, A. E. 1998, *A&AS*, **129**, 505.
Blanton, M. R., Roweis, Sam, 2007, *AJ*, **133**, 734.
Bohm-Vitense, E. 1980, *ARA&A*, **19**, 295.
Code, A. D., Davis, J., Bless, R. C., Hanbury-Brown, R. 1976, *ApJ*, **203**, 417.
Cuillandre, J. J., Withington, K., Hudelot, P., Goranova, Y., McCracken, H., Magnard, F., Mellier, Y., Regnault, N., Bétoule, M., Aussel, H., Kavelaars, J. J., Fernique, P., Bonnarel, F., Ochsenbein, F., Ilbert, O. 2012, SPIE, 8448, 0MC
Flower, P. J. 1996, *ApJ*, **469**, 355.
Girardi, L., Grebel, E. K., Odenkirchen, M., Chiosi, C. 2004, *A&A*, **422**, 205.
Gwyn, Stephen D. J. 2008, *PASP*, **120**, 212.
Gwyn, Stephen D. J. 2011, arXiv, **101**, 1084.
Hewett *et al*. 2006, *MNRAS*, **367**, 454.
Ivezic, Z., Sesar, B. *et al*. 2008, *ApJ*, **684**, 287.
Johnson, H. L. 1966, *ARA&A*, **4**, 193.
Lee *et al*. 2008, *AJ*, **136**, 2022.
Lejeune, T., Cuisinier, F., Buser, R. 1998, *A&AS*, **130**, 65.
Oke, J. B. 1974, *ApJS*, **27**, 210.
Pickles, A. J. *PASP* 110, **863**, 1998.
Pinsonneault, M. H., Terndrup, D. M., Hanson, R. B., Stauffer, J. R. 2004, *ApJ*, **600**, 946.
Ridgway, S. T., Joyce, R. R., White, N. M., Wing, R. F. 1980, *ApJ*, **235**, 126.
Schlegel, David J., Finkbeiner, Douglas P., Davis, Marc, 1998, *AJ*, **500**, 525.
Sekiguchi. M., Fukugita. M 2000, *AJ*, **120**, 1072.
Tsuji, T., Ohnaka, K., Aoki, W., Nakajima, T. 1996, *A&A*, **308**, L29.